RESEARCH ARTICLE

Co_3O_4/NiO@GQDs@SO_3H nanocomposite as high performance catalyst for the preparation of pyrimidines

Hossein Shahbazi-Alavi[1*], Ali Kareem Abbas[2], Javad Safaei-Ghomi[3]

[1] Young Researchers and Elite Club, Kashan Branch, Islamic Azad University, Kashan, Iran, Department of Organic Chemistry, Faculty of Chemistry, University of Kashan, Iran

[2] College of Applied Medical Sciences, University of Kerbala, Iraq

[3] Department of Organic Chemistry, Faculty of Chemistry, University of Kashan, Iran

ARTICLE INFO

Article History:
Received 13 Nov 2019
Accepted 21 Jan 2020
Published 1 Feb 2020

Keywords:
nanocomposite
one-pot
Heterogeneous catalysts
pyrimidine
nanoanalysis

ABSTRACT

Co_3O_4/NiO@GQDs@SO_3H nanocatalyst has been used as an effective catalyst for the preparation of 2,4-diamino-6-arylpyrimidine-5-carbonitrile derivatives through a three-component reaction of malononitrile, aromatic aldehydes and guanidine hydrochloride under reflux conditions in ethanol. The catalyst has been characterized by FT-IR, XRD, SEM, EDS, BET, TGA, XPS and VSM. Atom economy, reusable catalyst, low catalyst loading, applicability to a wide range of substrates and high yields of products are some of the notable features of this protocol.

How to cite this article
Shahbazi-Alavi H., Kareem Abbas A., Safaei-Ghomi J . Co_3O_4/NiO@GQDs@SO_3H nanocomposite as high performance catalyst for the preparation of pyrimidines. J. Nanoanalysis., 2020; 7(1): 52-61. DOI: 10.22034/jna.2019.1882952.1174.

INTRODUCTION

Pyrimidines show biological activities including anticancer [1], anti-inflammatory [2], anti-proliferative [3], anti-HIV [4] anti-bacterial [5], antihypertensive [6], antimalarial [7], antioxidant [8] and protein Kinase inhibitors [9]. These attributes make pyrimidines notable targets in organic synthesis for future consideration. A number of procedures have been developed for the preparation of pyrimidines using bismuth (III) nitrate pentahydrate [10], sodium hydroxide [11], potassium carbonate [12] and sodium acetate [13]. Despite the use of these ways, there remains a need for further new methods for the synthesis of pyrimidines. Graphene quantum dots (GQDs) are a novel member of carbon nanostructures that have quasi-spherical structures. GQDs have gained intensive attention owing to the remarkable features containing biological [14], biomedical [15], therapeutic applications [16], as a new class of photocatalysts [17], surfactants [18], electrochemical biosensing [19], an electrocatalytic activity [20], lithium battery application [21], optical properties and photovoltaic applications [22], photoluminescence [23-24]. bioimaging properties [25], and catalytic activity [26]. Potential applications of N-graphene quantum dots were recently reviewed on the basis of experimental and theoretical studies [27-30]. Synthesis of highly efficient nanocomposite catalysts for the synthesis of organic compounds is still a big challenge. To obtain larger surface area and more active sites, nanocatalysts are functioned by active groups [31-33]. It has been demonstrated that the decoration of the nanocatalyst with GQDs prevents the aggregation of fine particles and thus increases the effective surface area and number of reactive sites for an efficient catalytic reaction. The chemical groups on a GQD are able to catalyze chemical

* Corresponding Author Email: hossien_shahbazi@yahoo.com

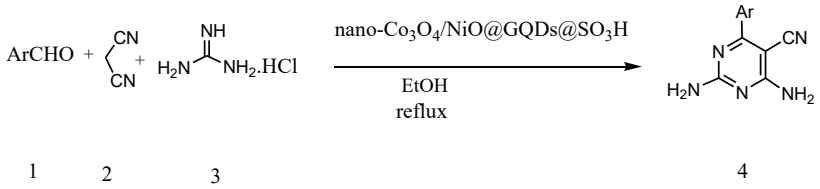

Scheme 1. The preparation of pyrimidines using Co_3O_4/NiO@GQDs@SO_3H nanocatalyst

reactions. The -COOH and -SO_3H groups can serve as acid catalysts for many reactions [26-34]. Nano catalyst/nanosorbents such as nano azido-selenenylation, nanomontmorillonite , MOF, MSN, nanocarbon structure(GO/G/MWCNTs) with different groups such as HS, NH_2, COOH and SO_3H, Cysteine and …, help for extraction cancer genic metals such as Cr, Pb, Hg from human body and use for drug delivery in cancer cells [35-38]. Herein, we reported the use of Co_3O_4/NiO@GQDs@SO_3H nanocomposite as a new efficient catalyst for the preparation of pyrimidines through a three-component reaction of malononitrile, aromatic aldehydes and guanidine hydrochloride (Scheme 1).

EXPERIMENTAL

Materials and characterization

Powder X-ray diffraction was taken on a Philips diffractometer of X'pert Company with monochromatized Cu Kα radiation (λ = 1.5406 Å). X-ray photoelectron spectroscopy (XPS) spectra were determined on an ESCA-3000 electron spectrometer. Microscopic morphology of nanocatalyst was performed by SEM (MIRA3). The thermogravimetric analysis (TGA) curves are gained by V5.1A DUPONT 2000. The magnetic measurement of samples was registered in a vibrating sample magnetometer (VSM) (Iran, Kashan Kavir). The surface area was carried out using nitrogen adsorption measurement (Micrometrics ASAP-2000).

Preparation of Co_3O_4/NiO nanoparticles

$Co(NO_3)_3$ and of $NiCl_2$ with 3:1 molar ratio was dissolved in ethylene glycol. Afterward, the appropriate amount of aqueous ammonia solution (28 wt%) was added to the above solution until the pH value reached 10. Then, transparent solution was placed in autoclave at 150 °C for 4h. The obtained precipitate was washed twice with methanol and dry at 60 °C for 8h. Finally, the product was calcined at 500 °C for 2h.

Preparation of Co_3O_4/NiO@N-GQDs nanocomposite

1 g citric acid and was dissolved into 20 mL deionized water, and stirred to form a clear solution. After that, 0.3 mL ethylenediamine was added to the above solution and mixed to obtain a clear solution. Then, 0.1 g Co_3O_4/NiO nanoparticles were added to the mixture. The mixture was stirred at room temperature within 5 minutes. Then the solution was transferred into a 50 ml Teflon lined stainless autoclave. The sealed autoclave was heated to 180°C for 12 hours in an electric oven. Finally, as-prepared nanostructured Co_3O_4/NiO@GQDs was obtained, washed several times with deionized water and ethanol, and then dried in an oven until constant weight was achieved.

Preparation of Co_3O_4/NiO@GQDs@SO_3H nanocomposite

1g of Co_3O_4/NiO@N-GQDs nanocomposite was dispersed in dry CH_2Cl_2 (10 mL) and sonicated for 5 min. Then, chlorosulfonic acid (0.8 mL in dry CH_2Cl_2) was added drop-wise to a cooled (ice-bath) mixture of Co_3O_4/NiO@N-GQDs, during a period of 30 min under N_2 with vigorous stirring. The mixture was stirred for 120 min, while the residual HCl was removed by suction with trapping. The resulted Co_3O_4/NiO@GQDs@SO_3H nanocomposite was separated, washed several times with dried CH_2Cl_2 before being dried under vacuum at 60 °C.

General procedure for the synthesis of pyrimidines

A mixture of malononitrile (1 mmol), aldehydes (1 mmol), guanidine hydrochloride (1 mmol) and Co_3O_4/NiO@GQDs@SO_3H nanocatalyst were stirred in 5 mL ethanol under reflux condition. The reaction was monitored by TLC. After completion of the reaction, the solution was filtered and the heterogeneous catalyst was recovered. Water was added, and the precipitate was collected by filtration and washed with water. The crude product was recrystallized or washed with ethanol to give the pure product. Spectra data 4c and 4d compounds are presented:

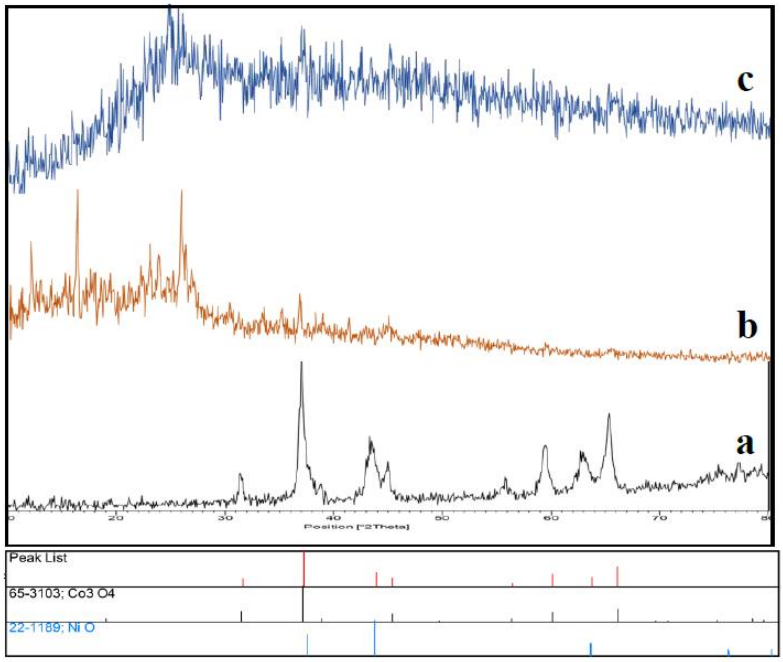

Fig 1. XRD pattern of (a) Co_3O_4/NiO, (b) Co_3O_4/NiO@GQDs and (c) Co_3O_4/NiO@GQDs @ SO_3H

2,4-diamino-6-(4-bromophenyl)pyrimidine - 5-carbonitrile (4c)

M. p. 261-263 °C. – IR (KBr): $\bar{\nu}$ = 3423, 3298 (NH_2), 2187 (CN), 1635, 1602, 1484 cm^{-1}. – ^1H NMR (400 MHz, DMSO-d_6): δ (ppm) = 6.84-6.90 (4H, 2 NH_2), 7.03-7.05 (2 H, J = 8 Hz, ArH), 7.11-7.14 (2 H, J = 8 Hz, ArH). – ^{13}C NMR(100 MHz, DMSO-d_6): δ (ppm) = 76.10, 118.37, 128.72, 130.42, 135.58, 136.20, 163.15, 165.30, 168.54. – Analysis for $C_{11}H_8BrN_5$: calcd. C 45.54, H 2.78, N 24.14; found: C 45.42, H 2.69, N 24.08.

2,4-diamino-6-(4-methoxyphenyl)pyrimidine- 5 -carbonitrile (4d)

M. p. 236-238 °C. – IR (KBr): $\bar{\nu}$ = 3385, 3325, 3284, 3205 (NH_2), 2202 (CN), 1646, 1482 cm^{-1}. – ^1H NMR (400 MHz, DMSO-d_6): δ (ppm) = 3.55 (3H, s, OCH_3), 7.57-7.64 (4H, 2 NH_2), 7.32 (2 H, m, ArH), 8.34 (2H, m, ArH). – ^{13}C NMR (100 MHz, DMSO-d_6): δ (ppm) = 54.32, 79.16, 113.42, 117.90, 125.64, 128.10, 160.22, 164.92, 167.44, 169.32. – Analysis for $C_{12}H_{11}N_5O$: calcd. C 59.74, H 4.60, N 29.03; found C 59.64, H 4.43, N 28.94.

RESULTS AND DISCUSSION

In the beginning, we prepared Co_3O_4/NiO nanoparticles by easy techniques. A facile hydrothermal method was used for the preparation of N-GQDs [39]. Sulfonated graphene quantum dots were prepared using chlorosulfonic acid [40]. XRD pattern of Co_3O_4/NiO, Co_3O_4/NiO@N-GQDs and Co_3O_4/NiO@GQDs @ SO_3H nanocomposite, is shown in Fig. 1. XRD pattern confirms presence of both NiO (JCPDS No.22-1189) and Co_3O_4 (JCPDS No 65-3103).

In order to investigate the particle size and morphology of nanoparticles, SEM image of Co_3O_4/NiO and Co_3O_4/NiO@ GQDs@SO_3H nanocomposite is indicated in Fig. 2. SEM images of the Co_3O_4/NiO@GQDs@SO_3H nanocomposite showed the formation of uniform particles, and the energy-dispersive X-ray spectrum (EDS) confirmed the presence of Co, Ni, O, S and C species in the structure of the nanocomposite (Fig. 3).

Magnetic properties of nanocomposites before and after their being decorated with GQDs were tested by vibrating-sample magnetometer (VSM) (Fig 4). The lower magnetism of the as-synthesized Co_3O_4/NiO@GQDs@SO_3H compared with the Co_3O_4/NiO was ascribed to the antiferromagnetic behavior of GQDs as a dopant. These results demonstrate that the magnetization property decreases by coating and functionalization [41-42].

FT-IR spectra of Co_3O_4/NiO, Co_3O_4/NiO@N-GQDs and Co_3O_4/NiO@GQDs @ SO_3H nanocomposite are shown in Fig. 5. The absorption

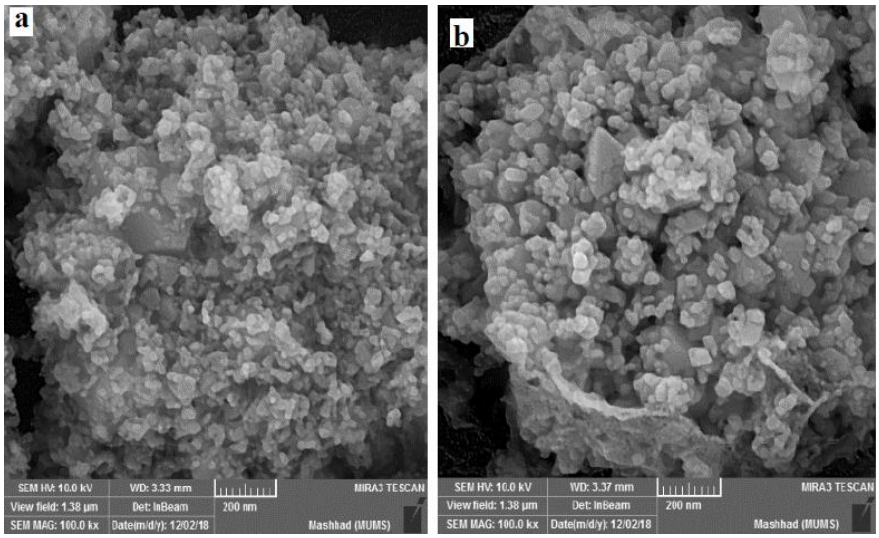

Fig 2. SEM image of (a) Co_3O_4/NiO, (b) Co_3O_4/NiO@GQDs @SO_3H

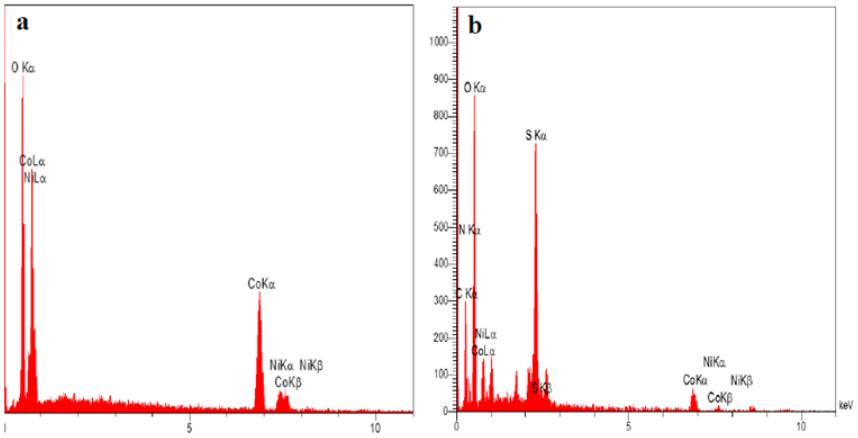

Fig 3. EDS spectrum of (a) Co_3O_4/NiO, (b) Co_3O_4/NiO@GQDs @SO_3H

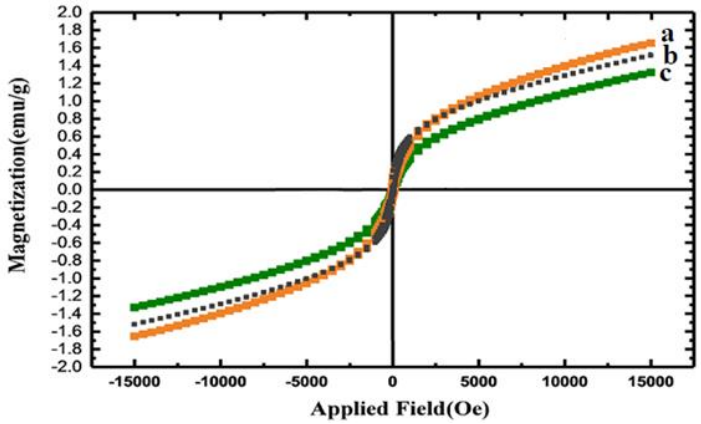

Fig 4. VSM of (a) Co_3O_4/NiO, (b) Co_3O_4/NiO@GQDs and (c) Co_3O_4/NiO@GQDs @SO_3H

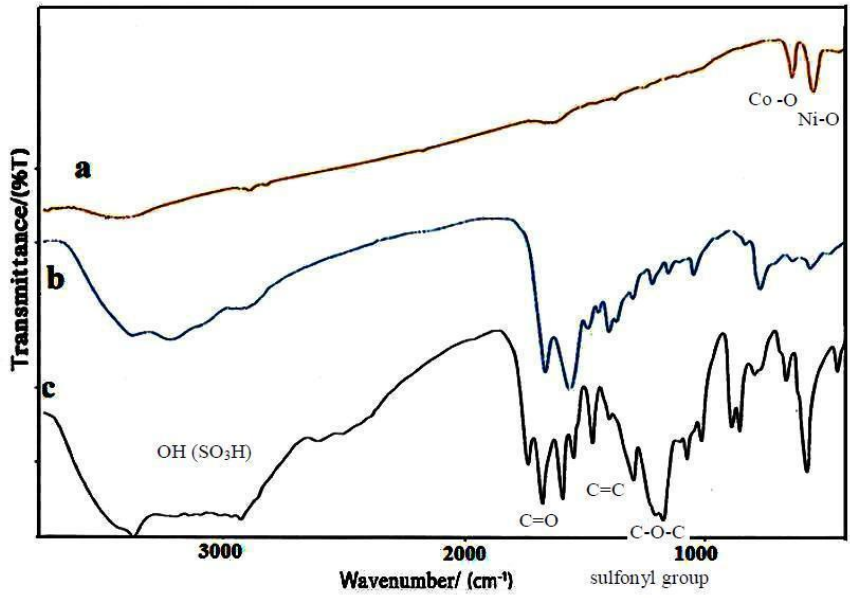

Fig 5. FT-IR of (a) Co_3O_4/NiO, (b) Co_3O_4/NiO@GQDs and (c) Co_3O_4/NiO@GQDs @SO_3H

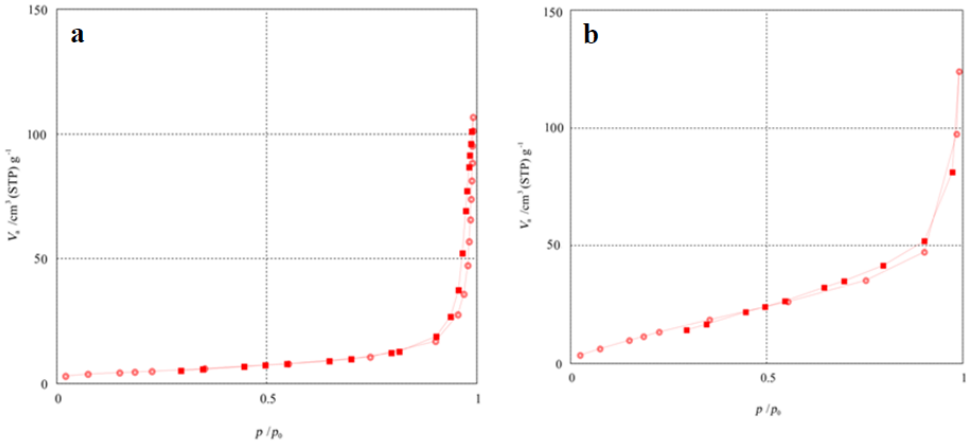

Fig 6. The BET specific surface area of (a) Co_3O_4/NiO, (b) Co_3O_4/NiO@GQDs @SO_3H

peak at 3335 cm^{-1} related to the stretching vibrational absorptions of OH. The peaks at 461.4, 568.4, 657.1 cm^{-1} corresponded to the Ni-O, Co^{+2}-O and Co^{3+}-O respectively. The characteristic peaks at 3440 cm^{-1} (O-H stretching vibration), 1705 cm^{-1} (C=O stretching vibration), 1125 cm^{-1} (C-O-C stretching, vibration) appear in the spectrum of Fig. 5b. The peak at approximately 1475-1580 cm^{-1} is attributed to C=C bonds. The presence of sulfonyl group is also verified by the peaks appeared at 1215 and 1120 cm^{-1}. The broad peak at 3350cm^{-1} related to the stretching vibrational absorptions of OH (SO_3H) (Fig 5c).

The BET specific surface area of Co_3O_4/NiO and Co_3O_4/NiO@GQDs@SO_3H nanocomposites was determined by the nitrogen gas adsorption-desorption isotherms (Fig. 6). The results presented that the BET specific surface area of Co_3O_4/NiO was improved from 12.25 to 32.43 m^2/g after modification with GQDs, therefore more active sites were introduced on Co_3O_4/NiO@GQDs@ SO_3H surface.

Thermal Analysis TGA (Thermogravimetric analysis) determines the thermal stability of the Co_3O_4/NiO@GQDs@SO_3H nanocomposite (Fig. 7). The curve indicates a weight loss about

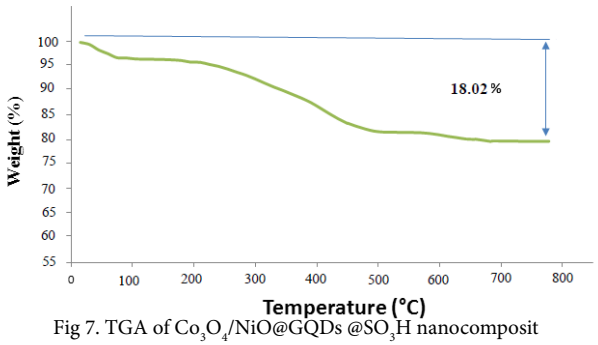

Fig 7. TGA of Co_3O_4/NiO@GQDs @SO_3H nanocomposit

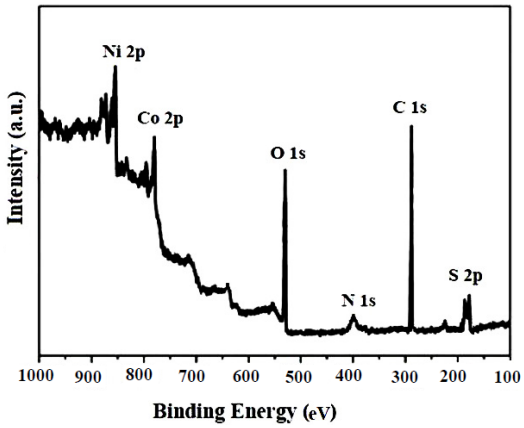

Fig. 8. X-ray photoelectron spectroscopy (XPS) analysis of Co_3O_4/NiO@GQDs@SO_3H nanocomposite

14.06 % from 150 to 500 °C, are attributed to the oxidation and degradation of GQD.

X-ray photoelectron spectroscopy (XPS) analysis of Co_3O_4/NiO@GQDs@SO_3H nanocomposite was indicated in Fig. 8. In the wide-scan spectrum of nanocatalyst, the predominant components are Ni $2p_{1/2}$ (873.4 eV), Ni $2p_{3/2}$ (854.4 eV), Co $2p_{1/2}$ (792.6 eV), Co $2p_{3/2}$ (780.4 eV), O 1s (529.8 eV), N 1s (400 eV), C 1s (284.5 eV) and S 2p (164.3 eV).

The concentration of sulfonic acid groups was quantitatively estimated by back titration using HCl (0.01 N). 2 mL of KOH (0.01 N) was added to 0.02 g of the nanoparticles and the mixture was stirred for 30 min. The catalyst was filtered and washed with deionized water. The excess amount of KOH was titrated with HCl (0.01 N) in the presence of phenolphthalein as indicator. Averages of 3 separate titrations were performed to obtain an average value for the acid amount of Co_3O_4/NiO@GQDs@SO_3H nanocomposite. The results revealed that the samples of Co_3O_4/NiO@GQDs@SO_3H nanocomposite possessed 0.82 mmol g-1 acid amount.

Initially, we carried out three-component reaction of malononitrile, benzaldehyde and guanidine hydrochloride as a model reaction. The model reaction was performed by Et_3N, $NaHSO_4$, ZrO_2, *p*-TSA, NiO, Co_3O_4, Co_3O_4/NiO, Co_3O_4/NiO@GQDs and Co_3O_4/NiO@GQDs@SO_3H nanocomposite. The reactions were tested using diverse solvents containing ethanol, acetonitrile, water and dimethylformamide. The best results were gained in EtOH and we found that the reaction gave convincing results in the presence of Co_3O_4/NiO@GQDs@SO_3H nanocomposite (4 mg) under reflux conditions (Tables 1).

A series of aromatic aldehydes were studied under optimum conditions (Table 2). The results were good in yields using aromatic aldehydes, either bearing electron-withdrawing substituents or electron-donating substituents. The influence of electron-withdrawing and electron-donating substituents on the aromatic ring of aldehydes upon the reaction yields was investigated. Aromatic aldehydes having NO_2 and halogen groups reacted at faster rate compared with aromatic aldehydes

Table1: Optimization of reaction condition using different catalysts [a]

Entry	Catalyst (amount)	Solvent (reflux)	Time (min)	Yield %
1	none	EtOH	300	NR
2	Et_3N (5 mol%)	EtOH	300	38
3	$NaHSO_4$ (4 mol%)	EtOH	250	42
4	ZrO_2 (4 mol%)	EtOH	150	50
5	*p*TSA (5 mol%)	EtOH	150	55
6	Nano-Co_3O_4	EtOH	150	48
7	Nano-NiO	EtOH	150	58
8	Co_3O_4/NiO nanocomposite	EtOH	150	64
9	Co_3O_4/NiO@GQDs nanocomposite	EtOH	150	74
10	Co_3O_4/NiO@GQDs@SO_3H nanocomposite (2 mg)	EtOH	30	85
11	Co_3O_4/NiO@GQDs@SO_3H nanocomposite (4 mg)	EtOH	30	92
12	Co_3O_4/NiO@GQDs@SO_3H nanocomposite (6 mg)	EtOH	30	92
13	Co_3O_4/NiO@GQDs@SO_3H nanocomposite (4 mg)	H_2O	50	68
14	Co_3O_4/NiO@GQDs@SO_3H nanocomposite (4 mg)	DMF	50	73
15	Co_3O_4/NiO@GQDs@SO_3H nanocomposite (4 mg)	CH_3CN	50	80

[a] Reaction conditions: benzaldehyde (1 mmol), malononitrile (1 mmol), and guanidine hydrochloride (1 mmol); [b] isolated yield

Table 2: Synthesis of pyrimidines using Co_3O_4/NiO@GQDs@SO_3H nanocomposite (4 mg)

Entry	Product	Ar	Time (min)	yield (%)	m.p. (°C)
1	**4a**	C_6H_5	30	92	237-239
2	**4b**	4-Cl-C_6H_4	25	93	265-267
3	**4c**	4-Br-C_6H_4	25	94	260-262
4	**4d**	4-OMe-C_6H_4	40	84	236-238
5	**4e**	4-Me-C_6H_4	40	86	255-257
6	**4f**	2,6-di-Cl-C_6H_4	25	94	275-276
7	**4g**	2-Cl-C_6H_4	30	93	232-235
8	**4h**	3-Me- C_6H_4	40	88	225-227
9	**4i**	NO_2	25	96	252-254
10	**4j**	CN	25	94	242-244

[a] isolated yield

substituted with other groups.

To compare the efficiency of Co_3O_4/NiO@GQDs@SO_3H nanocomposite with the reported catalysts for the synthesis of pyrimidines, we have tabulated the results in Table 3. As Table 3 indicates, Co_3O_4/NiO@GQDs@SO_3H nanocomposite is superior with respect to the reported catalysts in terms of reaction time, yield and conditions. Atom

Table 3. Comparison of catalytic activity of Co_3O_4/NiO@GQDs@SO_3H nanocomposite with other reported catalysts

Entry	catalyst	Time (min)	Yield,[a] %	[Ref]
1	Sodium acetate (20 mol%)	300	78	[9]
2	Potassium carbonate (10 mol%)	180	75	[8]
3	Sodium hydroxide (20 mol%)	30	88	[7]
4	Co_3O_4/NiO@GQDs@SO_3H nanocomposite (4 mg)	30	92	This work

[a] Isolated yield

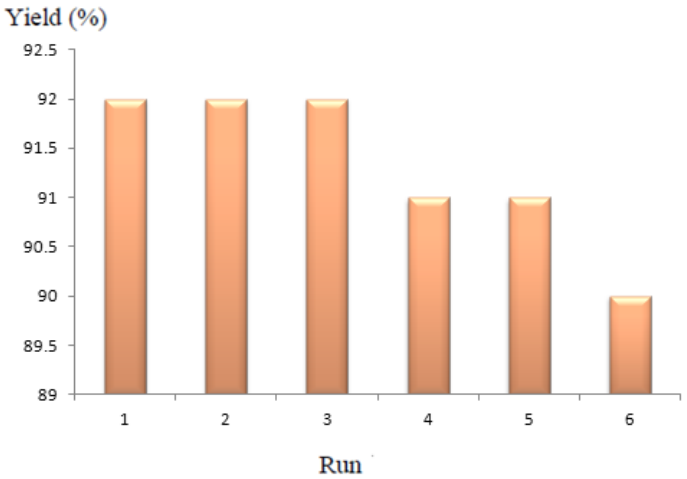

Fig. 9. Recycling of Co_3O_4/NiO@GQDs @SO_3H nanocomposite as catalyst for the model reaction

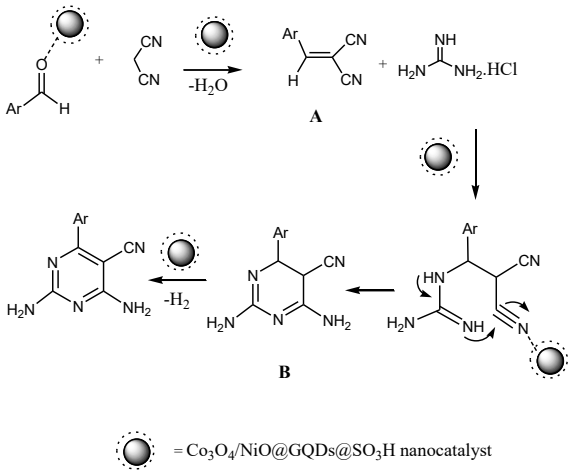

Scheme 2: Possible mechanism for the synthesis of pyrimidines using Co_3O_4/NiO@GQDs@SO_3H nanocatalyst

economy, reusable catalyst, low catalyst loading, applicability to a wide range of substrates and high yields of products are some of the notable features of this protocol.

We also determined recycling of Co_3O_4/NiO@GQDs@SO_3H nanocomposite as catalyst for the model reaction under reflux conditions in ethanol. The results showed that nanocomposite can be reused several times without noticeable loss of catalytic activity (Yields 92 to 90%) (Fig. 9).

A plausible mechanism for the preparation of pyrimidines using Co_3O_4/NiO@GQDs@SO_3H nanocomposites is indicated in Scheme 2. Firstly, the reaction occurs by formation of the cyano

olefin **A** from the condensation of malononitrile and aryl aldehyde. The second step is followed by Michael addition, cycloaddition, isomerization, aromatization to afford the pyrimidines. The SO_3H groups distributed on the surface of Co_3O_4/NiO@ GQDs activate the C=O and C≡N groups for better reaction with nucleophiles.

CONCLUSION

In this study, we described the preparation of pyrimidines using Co_3O_4/NiO@GQDs@SO_3H nanocomposite as a superior catalyst under reflux conditions. The SO_3H groups distributed on the surface of Co_3O_4/NiO@GQDs activate the C=O and C≡N groups for better reaction with nucleophiles. The current method provides obvious positive points containing environmental friendliness, significantly shorter reaction time, the reusability of the catalyst, low catalyst loading and simple work-up procedure.

ACKNOWLEDGMENT

The authors are grateful to the University of Kashan for supporting this work under grant no. 159148/XII.

CONFLICT OF INTEREST

The authors declare that there is no conflict of interests regarding the publication of this manuscript.

REFERENCES

1. G. Luo, Z. Tang, K. Lao, X. Li, Q. You, H. Xiang, Structure-activity relationships of 2, 4-disubstituted pyrimidines as dual ERα/VEGFR-2 ligands with anti-breast cancer activity. Eur. J. Med. Chem. 2018, 150:783-795.
2. G.N. Tageldin, S.M. Fahmy, H.M. Ashour, M.A. Khalil, R.A. Nassra, I.M. Labouta, Design, synthesis and evaluation of some pyrazolo[3,4-d]pyrimidines as anti-inflammatory agents. Bioorg. Chem. 2018, 78:358-371.
3. E. Dreassi, A.T. Zizzari, M. Mori, I. Filippi, A. Belfiore, A. Naldini, F. Carraro, A. Santucci, S. Schenone, M. Botta, 2-Hydroxypropyl-β-cyclodextrin strongly improves water solubility and anti-proliferative activity of pyrazolo[3,4-d] pyrimidines Src-Abl dual inhibitors. Eur. J. Med. Chem. 2010, 45:5958-5964.
4. Z. Hajimahdi, A. Zarghi, R. Zabihollahi, M.R. Aghasadeghi, Synthesis, biological evaluation, and molecular modeling studies of new 1,3,4-oxadiazole- and 1,3,4-thiadiazole-substituted 4-oxo-4H-pyrido[1,2-a]pyrimidines as anti-HIV-1 agents, Med. Chem. Res. 2013, 22:2467-2475.
5. S. Rostamizadeh, M. Nojavan, R. Aryan, H. Sadeghian, M. Davoodnejad, A novel and efficient synthesis of pyrazolo [3, 4-d] pyrimidine derivatives and the study of their anti-bacterial activity. Chin. Chem. Lett. 2013, 24:629-632.
6. L.R. Bennett, C.J. Blankley, R.W. Fleming, R.D. Smith, D.K. Tessman, Antihypertensive activity of 6-arylpyrido [2, 3-d] pyrimidin-7-amine derivatives, J. Med. Chem. 1981, 24:382-389.
7. S. Manohar, U.C. Rajesh, S.I. Khan, B.L. Tekwani, D.S. Rawat, Novel 4-aminoquinoline-pyrimidine based hybrids with improved in vitro and in vivo antimalarial activity, ACS Med. Chem. Lett. 2012, 3:555-559.
8. Y. Kotaiah, N. Harikrishna, K. Nagaraju, C. Venkata Rao, Synthesis and antioxidant activity of 1, 3, 4-oxadiazole tagged thieno [2, 3-d] pyrimidine derivatives, Eur. J. Med. Chem. 2012, 58:340-345.
9. S. Schenone, M. Radi, F. Musumeci, C. Brullo, M. Botta, Biologically driven synthesis of pyrazolo[3,4-*d*]pyrimidines as protein kinase inhibitors: an old scaffold as a new tool for medicinal chemistry and chemical biology studies. Chem. Rev. 2014, 114:7189–7238.
10. M. Zahedifar, H. Sheibani, Rapid three-component synthesis of pyrimidine and pyrimidinone derivatives in the presence of $Bi(NO_3)_3.5H_2O$ as a mild and highly efficient catalyst. Res. Chem. Intermed. 2015, 41:105-111.
11. Q. Zhuang, H. X. Han, S. Wang, S. Tu, L. Rong, Efficient and facile three-component reaction for the synthesis of 2-amine-4,6-diarylpyrimidine under solvent-free conditions. Synth. Commun. 2009, 39:516–522.
12. M. B. Deshmukh, P. V. Anbhule, S. D. Jadhav, S. S. Jagtap, D. R. Patil, S. M. Salunkhe, S. A. Sankpal, A novel and environmental friendly, one-step synthesis of 2, 6-Diamino-4-phenyl pyrimidine-5-carbonitrile using potassium carbonate in water. Indian J. Chem. B. 2008, 47:792-795.
13. H. Sheibani, A.S. Saljoogi, A. Bazgir, Three-component process for the synthesis of 4-amino-5-pyrimidinecarbonitriles under thermal aqueous conditions or microwave irradiation. Arkivoc, 2008, 2008 (ii):115-123.
14. X.T. Zheng, A. Ananthanarayanan, K.Q. Luo, P. Chen, Glowing graphene quantum dots and carbon dots: properties, syntheses, and biological applications. small, 2015, 11:1620–1636.
15. B. Senel, N. Demir, G. Büyükköroglu, M. Yildiz, Graphene quantum dots: Synthesis, characterization, cell viability, genotoxicity for biomedical applications. Saudi. Pharm. J. 2019, 27:846-858.
16. M.J. Molaei, Carbon quantum dots and their biomedical and therapeutic applications: a review. RSC Adv., 2019, 9:6460- 6481.
17. T.F. Yeh, C.Y. Teng, S.J. Chen, H. Teng, Nitrogen-doped graphene oxide quantum dots as photocatalysts for overall water-splitting under visible light Illumination. Adv. Mater. 2014, 26:3297–3303.
18. F. Xi, J. Zhao, C. Shen, J. He, J. Chen, Y. Yan, K. Li, J. Liu, P. Chen, Amphiphilic graphene quantum dots as a new class of surfactants. Carbon, 2019, 153:127-135.
19. Y. Wang, Y. Shao, D.W. Matson, J. Li, Y. Lin, Nitrogen-doped graphene and its application in electrochemical biosensing. ACS Nano 2010, 4:1790-1798.
20. Q. Li, S. Zhang, L. Dai, L.S. Li, Nitrogen-doped colloidal graphene quantum dots and their size-dependent electrocatalytic activity for the oxygen reduction reaction. J. Am. Chem. Soc. 2012, 134:18932-18935.
21. A.L.M. Reddy, A. Srivastava, S.R. Gowda, H. Gullapalli, M. Dubey, P.M. Ajayan, Synthesis of nitrogen-doped graphene films for lithium battery application. ACS Nano 2010, 4:6337-6342.
22. M.T. Hasan, R. Gonzalez-Rodriguez, C. Ryan, K. Pota, K.

Green, J.L. Coffer, A.V. Naumov, Nitrogen-doped graphene quantum dots: Optical properties modification and photovoltaic applications. Nano Res. 2019, 12:1041-1047.
23. F. Temerov, A. Beliaev, B. Ankudze, T.T. Pakkanen, Preparation and photoluminescence properties of graphene quantum dots by decomposition of graphene-encapsulated metal nanoparticles derived from Kraft lignin and transition metal salts. J. Lumin. 2019, 206:403-411.
24. S. Zhu, Y. Song, X. Zhao, J. Shao, J. Zhang, B. Yang, The photoluminescence mechanism in carbon dots (graphene quantum dots, carbon nanodots, and polymer dots): current state and future perspective. Nano Res. 2015, 8:355-381.
25. D. Qu, M. Zheng, J. Li, Z. Xie, Z. Sun, Tailoring color emissions from N-doped graphene quantum dots for bioimaging applications. Light Sci Appl. 2015, 4:364-371.
26. S. Sajjadi, A. Khataee, R.D.C. Soltani, A. Hasanzadeh, N, S co-doped graphene quantum dot–decorated Fe_3O_4 nanostructures: Preparation, characterization and catalytic activity. J. Phys. Chem. Solids, 2019, 127:140-150.
27. Y. Du, S. Guo, Chemically doped fluorescent carbon and graphene quantum dots for bioimaging, sensor, catalytic and photoelectronic applications. Nanoscale, 2016, 8:2532-2543.
28. Y. Yan, J. Gong, J. Chen, Z. Zeng, W. Huang, K. Pu, J. Liu, P. Chen, Recent advances on graphene quantum dots: from chemistry and physics to applications. Adv. Mater. 2019, 31:1808283-1808305.
29. M. Li, T. Chen, J.J. Gooding, J. Liu, Review of carbon and graphene quantum dots for sensing. ACS Sens. 2019, 4:1732-1748.
30. Z. Wang, H. Zeng, L. Sun, Graphene quantum dots: versatile photoluminescence for energy, biomedical, and environmental applications. J. Mater. Chem. C, 2015, 3:1157-1165.
31. E. Hu, X.Y. Yu, F. Chen, Y. Wu, Y. Hu, X. Wen, D. Lou, Graphene Layers-Wrapped Fe/Fe_5C_2 Nanoparticles Supported on N-doped Graphene Nanosheets for Highly Efficient Oxygen Reduction. Adv. Energy Mater. 2018, 8:1702476-1702483.
32. P.B. Koli, K.H. Kapadnis, U.G. Deshpande, M.R. Patil, Fabrication and characterization of pure and modified Co_3O_4 nanocatalyst and their application for photocatalytic degradation of eosine blue dye: a comparative study, J. Nanostructure Chem. 2018, 4:453-463.
33. E. Hu, Y. Feng, J. Nai, D. Zhao, Y. Hu, X. Wen, D. Lou, Construction of hierarchical Ni–Co–P hollow nanobricks with oriented nanosheets for efficient overall water splitting. Energy Environ. Sci., 2018, 11:872-880.
34. E. Hu, J. Ning, B. He, Z. Li, C. Zheng, Y. Zhong, Z. Zhang, Y. Hu, Unusual formation of tetragonal microstructures from nitrogen-doped carbon nanocapsules with cobalt nanocores as a bi-functional oxygen electrocatalyst. J. Mater. Chem. A, 2017, 5:2271-2279.
35. M. Gou, B.B. Yarahmadi, Separation and determination of lead in human urine and water samples based on thiol functionalized mesoporous silica nanoparticles packed on cartridges by micro column fast micro solid-phase extraction, Anal. Method Environ. Chem. J. 2019, 2:39-50.
36. A. Ghozatloo, Modification of graphene for speciation of chromium in wastewater samples by suspension solid phase microextraction procedure, Anal. Method Environ. Chem. J. 2019, 2:51-66.
37. F.S. Ebnerasool, N.M. Kazemi, Preparation and characterization of chitosan nanocomposite based on nanoscale silver and nanomontmorillonite, Anal. Meth. Environ. Chem. J., 2019, 2:5-12.
38. A. Rouhollahi, Z. Asghari, B. Movassagh, Analytical Methods: Electrochemical azido-selenenylation of some olefins by cyclic voltammetry and controlled-potential coulometry, Anal. Meth. Environ. Chem. J., 2018, 1:67-74.
39. D. Qu, M. Zheng, P. Du, Y. Zhou, L. Zhang, D. Li, H. Tan, Z. Zhao, Z. Xie, Z. Sun, Highly luminescent S, N co-doped graphene quantum dots with broad visible absorption bands for visible light photocatalysts. Nanoscale, 2013, 5:12272-12277.
40. K. Li, J. Chen, Y. Yan, Y. Min, H. Li, F. Xi, J. Liu, P. Chen, Quasi-homogeneous carbocatalysis for one-pot selective conversion of carbohydrates to 5-hydroxymethylfurfural using sulfonated graphene quantum dots. Carbon, 2018, 136: 224-233.
41. N. Limchoowong, P. Sricharoen, Y. Areerob, P. Nuengmatcha, T. Sripakdee, S. Techawongstien, S. Chanthai, Preconcentration and trace determination of copper (II) in Thai food recipes using Fe3O4@ Chi–GQDs nanocomposites as a new magnetic adsorbent. Food Chem. 2017, 230:388–397.
42. H. Shahbazi-Alavi, J. Safaei-Ghomi, Cross-linked sulfonated polyacrylamide (Cross-PAA-SO_3H) attached to nano-Fe_3O_4 as a superior catalyst for the synthesis of oxindoles, J. Nanoanalysis., 2019, 6:185-192.